Energy 156 (2018) 169–180

Contents lists available at ScienceDirect

Energy

journal homepage: www.elsevier.com/locate/energy

Comparative thermodynamic evaluation of a geothermal power plant by using the advanced exergy and artificial bee colony methods

Osman Özkaraca [a], Ali Keçebaş [b, *], Cihan Demircan [c]

[a] Department of Information Systems Engineering, Technology Faculty, Muğla Sıtkı Koçman University, 48000 Muğla, Turkey
[b] Department of Energy Systems Engineering, Technology Faculty, Muğla Sıtkı Koçman University, 48000 Muğla, Turkey
[c] Department of Energy Systems Engineering, Graduate School of Natural and Applied Sciences, Süleyman Demirel University, 32260 Isparta, Turkey

ARTICLE INFO

Article history:
Received 27 November 2017
Received in revised form
8 April 2018
Accepted 13 May 2018
Available online 15 May 2018

Keywords:
Geothermal power plant
Thermal performance improvement
Optimization
Advanced exergy analysis
Artificial bee colony

ABSTRACT

In this study, the thermodynamic performance of a binary geothermal power plant (GPP) is comparatively evaluated using the exergy analysis and optimization method. Thus, in addition to routes to improve the thermodynamic performance of the system, the thermodynamic relationships between the system components and improvement performances of the components are determined. With this aim, the Sinem GPP located in Aydın province in Turkey as a real system is selected. All data from the system are collected and a numerical model simulating the real system is developed. On the developed model, the conventional and advanced exergy analyses for exergy analysis and the artificial bee colony (ABC) method for optimization process are performed. The results of the study show that total exergy efficiencies of the conventional exergy analysis, advanced exergy analysis and artificial bee colony are determined as 39.1%, 43.1% and 42.8%, respectively. The exergy efficiency obtained from advanced exergy analysis is higher compared to the other two methods. This is due to the fact that theoretical and unavoidable operation assumptions in advanced exergy analysis are arbitrary as a single value depending on the decision maker. However, decision variables in the ABC method are within certain constraints chosen by the decision maker. It is better to select constraint limits instead of an arbitrary single value selection. Therefore, its arbitrary values should be confirmed with any optimization method. Additionally, the highest exergy destruction identified in the three methods is occurred in heat exchangers as the condenser and vaporizer.

1. Introduction

Energy forms one of the most important and basic requirements for the economic and social life of humans and countries through the ages. As a result, energy needs to be clean, cheap, uninterrupted, reliable and diversified supply [1]. Currently energy is obtained both from fossil resources and renewable resources. The use of renewable energy resources has become mandatory as fossil based energies will run out within a certain period, production from new reserves is very expensive and it harms the environment. Therefore, in the 21st century energy production from renewable energy resources has focused on biomass, solar, wind energies and to a lesser extent on hydraulic energy [2]. However, the basic problem related to renewable energy resources is that they are not baseload power generation. Traditionally the most important responsibility of thus systems is baseload providers, which are power plants able to generate a fixed and predictable supply of electricity [3]. The primary energy source in the majority of electricity networks are baseload electricity power plants using fossil fuels [4]. The renewable energy resources such as geothermal and biomass energies are the only renewable energy resources that is not affected by external weather conditions. Thus, geothermal and biomass energies may be used as a basic energy source [1]. However, this article focuses on geothermal energy.

Geothermal energy is heat energy carried to the surface as hot water and steam formed due to heat accumulated at a variety of depths within the crust with temperatures continuously above the mean regional atmospheric temperature and containing higher amounts of dissolved minerals, a variety of salts and gases compared to normal underground and surface water in the environment [5]. Geothermal energy resources are therefore used linked to their temperature. Generally high temperature

* Corresponding author.
E-mail address: alikecebas@gmail.com (A. Keçebaş).

https://doi.org/10.1016/j.energy.2018.05.095
0360-5442/

($T > 150\,^{\circ}C$) resources are used for electricity production, with moderate ($90\,^{\circ}C < T < 150\,^{\circ}C$) and low temperature ($T < 90\,^{\circ}C$) resources are used in direct use fields such as bathing, individual and district heating and cooling etc. [6]. In recent times, very low temperature ($T < 35\,^{\circ}C$) resources have been used in heat pump applications. Additionally the latest researches have stated that while the global geothermal installed power capacity was 1.3 GW in 1975, in 2010 this had risen to 10.9 GW and then to 12.7 GW in 2015. Since 2015, nearly 3.45 GW of the installed power of 12.7 GW was installed in the USA. There was a 17% increase in global geothermal installed power and a 10% increase in electricity production in 2015 compared to 2010. In 2020 it is estimated the installed power will be about 21 GW [6]. According to Bertani [6], the top 5 countries with highest geothermal installed power and electricity production globally may be listed as USA, Philippines, Indonesia, Mexico and New Zealand. In Turkey the installed power from geothermal energy was 19 MW in 2005, while this had risen to 624 MW in 2015. Currently this value has reached nearly 821 MW. According to Turkey's Energy Atlas, the 32 geothermal power plants in Turkey reached a total installed power of 921.5 MW and corresponded to 1.2% of the 78497.4 MW installed power in Turkey at the end of 2016 [7]. Thus while the development of geothermal power continues to meet the increasing electricity demands in the USA and globally, engineers and policy makers require data about feasibility and optimum design of geothermal energy power plants within a spectrum of geothermal resource conditions and climates. Therefore, there is a need for this type of scientifically robust design, analysis and optimization guidelines.

In spite of the disadvantages of geothermal power plants, due to the limitations of primary energy resources and rapid increase in energy costs, the importance of energy analyses to determine the energy losses of these and many thermal systems is increased. One of the important roles of energy analysis within development of energy systems is to ensure the energy system designers and operators have the necessary information. After the oil crisis occurring in the 1970s, it was understood that energy analysis alone did not reveal how effectively energy was used. Thus, exergy analyses began to gain great importance [8]. However, through the conventional exergy analysis, one cannot assess the mutual interdependencies among the system components neither the real potential for improving the components. This may be possible in an advanced exergetic analysis [9]. In recent times, very few researchers have used advanced exergy analysis for a variety of geothermal power plants [10–12]. In regard, this paper will comparatively evaluate the thermodynamic performance of a binary geothermal power plant using conventional and advanced exergy analyses and the artificial bee colony optimization method.

There are many studies about application of various optimization methods in thermodynamic cycles of any energy conversion system. Dai et al. [13] conducted the thermodynamic optimization of an organic Rankine cycle (ORC) with low grade waste heat recovery using different working fluids with exergy efficiency as the objective function by means of the genetic algorithm (GA). They reported that the ORC system with R236EA had higher exergy efficiency compared with other working fluids (e.g., ammonia, isobutene, R11, water). Sun et al. [14] proposed a ROSENB optimization algorithm combining with penalty function method to search the optimal set of operating variables to maximize either the net power generation or the thermal efficiency. They investigated the effects of working fluid mass flow rate, air cooled condenser fan air mass flow rate and expander inlet pressure on the system thermal efficiency and system net power generation. Rashidi et al. [15] conducted a parametric study and optimization of regenerative ORC with two feedwater heaters with thermal efficiency, exergy efficiency and specific work as the objective functions by means of artificial neural network (ANN) and artificial bee colony (ABC). They found that the maximum values of the specific network, the thermal efficiency and the exergy efficiency for R717 were greater than those for water. Arslan and Yetik [16] optimized a supercritical ORC-Binary geothermal power plant in the Simav region using ANN for economic costs. Arslan [17] completed a similar study in a geothermal-sourced Kalina power cycle. Wang et al. [18] used the non-dominated sorting genetic algorithm-II (NSGA-II) to increase the thermodynamic and economic performance of a low grade waste heat recovery organic Rankine cycle. Besides, the effects of turbine inlet pressure, turbine inlet temperature, pinch temperature difference, approach temperature difference and condenser temperature difference on the exergy efficiency and overall capital cost were investigated. They found that the optimum exergy efficiency and overall capital cost were 13.98% and 1292800 USD, respectively. Clarke et al. [19] compared the limited, non-linear simulation-based optimization of a double flash geothermal energy power plant using GA and particle swarm optimization (PSO) performance. Another study by Clarke and McLeskey Jr [20] used a multi-objective PSO method for the Pareto-optimal set used in the design of a power plant to determine the optimum use of the superheater and/or recuperator in a binary geothermal electricity power plant at environmental temperatures and brine temperatures. Karadas [21] used the true design parameters of the Dora 1 GPP located in Turkey to design an air-cooled, binary fluid geothermal power plant and investigated the effect of the design parameters on the theoretical power plant performance. Additionally, to be able to assess the power plant performance, they used real data from the Dora 1 GPP for regression analysis. Using three measurable independent variables such as ambient air temperature, flow rate and temperature of geofluid, they developed multiple annual linear regression models from 2006 to 2012. Saffari et al. [22] used the ABC method to optimize the thermal efficiency of a low temperature Kalina cycle with double turbine. Additionally, the study researched the effects of the entry pressure and temperature of the separator, basic ammonia mass fraction and basic mass flow rate of the working fluid on the net power output and thermal efficiency of the cycle. They reported that the proposed Kalina cycle had a thermal efficiency of 26.32%. Another study by Saffari et al. [23] assessed the thermodynamic performance of the Husaviv power plant with a Kalina cycle using the ABC optimization method. With the aim of identifying a more rapid and sensitive optimization of this system, they compared the ABC method with the GA, PSO and differential evolution (DE) methods. They researched the effects of parameters like entry temperature, pressure and mass flow rate of separator and basic ammonia mass fraction on the energy and exergy efficiencies of the system. They found the energy and exergy efficiencies of the system were 20.36% and 48.18%, respectively. They showed again in this study that the ABC method is more useable compared to the other methods. Proctor et al. [24] developed a dynamic model of a commercial scale geothermal ORC and confirmed this with power plant data. The standard deviation between the model and real power plant for output power and mean output power was between 1.4% and 0.24%, respectively. Li et al. [25] performed quantitative analysis of non-design performance for a low temperature geothermal resource using a Kalina cycle. In this study the non-design models including the turbines, pump and heat exchangers were previously created. To maximize the net output power and determine thermodynamic parameters in the design stage, they used the GA method. Wu et al. [26] presented and analysed the transcritical power cycles used for a CO_2-based binary zeotropic mixtures with temperatures of cooling water of 10–30 °C and low grade geothermal fluid of 100–150 °C. Under these conditions, 6 coolants were chosen to be added to CO_2. The transcritical power cycle performances with the 6 chosen CO_2-based mixtures were optimized with the pattern search algorithm (PSA). The thermodynamic and economic analyses were performed. In terms of thermal and economic performances, the best working fluid for the transcritical power cycle was R161/CO_2 and as the thermal performance of R290/CO_2 is low, it was determined not to be an appropriate working fluid for transcritical power cycles.

When the literature is carefully scanned, the number of studies using both conventional (CExA) and advanced (AExA) exergy analyses and the optimization method (ABC) to maximize the exergy efficiency of an energy conversion system as a single-objective function are very low. In this study for first time, the exergy efficiency of a geothermal power system will be optimized with the ABC method and additionally the thermodynamic performance of the geothermal power plant will be assessed comparatively with the results of each method (CExA, AExA and ABC). In this way the aim is to obtain further information for thermal system engineers and designers to use while maximizing the exergy efficiency of a geothermal power plant or while improving the system. The rest of paper is organized as follows. In Section 2, the description of the system, the thermodynamic modelling, the analysis and optimization processes, and the single objective function are given. The results of the CExA and AExA analyses and the ABC optimization method used to maximize the system exergy efficiency are discussed in Section 3 and finally, the paper is concluded in Section 4.

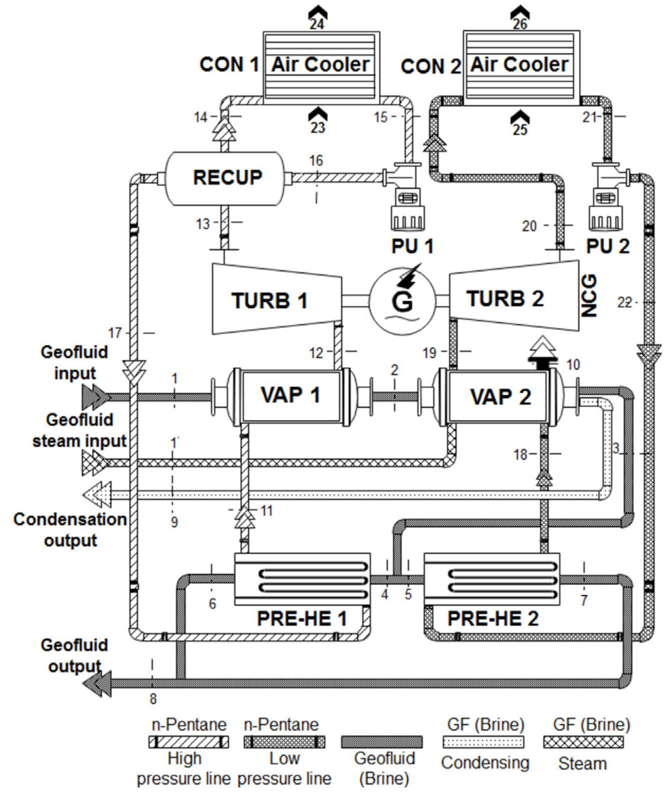

Fig. 1. The schematic flow diagram of the Sinem GPP.

2. Material and methods

2.1. Description of the system

The high temperature geothermal fields in Turkey are located in the Büyük Menderes basin continental rift belt. One of these fields is the nearly 116 MW capacity Hıdırbeyli region in Germencik county within the boundaries of Aydın province/Turkey. The Sinem GPP operating at 24 MW installed power in this geothermal field was chosen. This GPP is an air-cooled, two level binary organic Rankine cycle power plant. The GPP is designed to operate using geofluid with 165 °C, 1040 kPa and 445 kg/s and its steam with the same temperature and pressure and flow rate of 8.33 kg/s from separators. Then at the exit of the power plant the waste geofluid is pumped at 85 °C and 590 kPa pressure to re-injection wells. In addition, of this steam 30% comprises non-condensable gases (NCG). The schematic flow diagram of the Sinem GPP is illustrated in Fig. 1. In this study it is used operating parameters (pressure, temperature and mass flow rate) from the available Sinem GPP shown in the state numbers specified in Fig. 1 that were collected from the Supervisory Control System (SCADA) program of the system on April 14, 2013. The environmental temperature and pressure on that date were recorded as 25 °C and 1 bar.

2.2. Thermodynamic modelling

Actually operated Sinem GPP system is divided into some control volumes and the thermodynamic balance equations are applied to these control volumes. These control volumes are the vaporizers (VAP 1 and VAP 2) and preheaters (PRE-HE 1 and PRE-HE 2) performing heat exchange between the geofluid and the working fluid of *n*-pentane, the condensers (CON 1 and CON 2) performing heat exchange between air and *n*-pentane, and the recuperator (RECUP), turbines (TURB 1 and TURB 2) and pumps (PU 1 and PU 2) using only *n*-pentane. The thermodynamic properties of water instead of the geothermal fluid (brine) [27], the working fluid of *n*-pentane and the ideal gas of air for each control volume are calculated using the COOLPROP program [28,29] and thermodynamic balance equations and numerical calculations are completed with the MATLAB program [30]. In this way the thermodynamic fluid properties in the COOLPROP can be recalled on coded function in the MATLAB. An algorithm is developed using the MATLAB platform for the thermodynamic analysis and modelling of the real Sinem GPP. In addition, the balance equations for every component of a binary GPP with ORC as the Sinem GPP can be found in Ref. [10–12,20,21,24]. However, for the sake of simplicity the balance equations used in the thermodynamic modelling of the system are given in brief in the text.

Generally ignoring the changes in kinetic and potential energies, the mass and energy balances may be stated as follows

$$\sum \dot{m}_{in} = \sum \dot{m}_{out} \tag{1}$$

$$\dot{Q} + \sum \dot{m}_{in} h_{in} = \dot{W} + \sum \dot{m}_{out} h_{out} \tag{2}$$

where $\dot{m}$ is the mass flow rate, $\dot{Q} = \dot{Q}_{net,in}$ is the net heat input rate, $\dot{W} = \dot{W}_{net,out}$ is the work output rate, and h is the specific enthalpy.

The conventional exergy balance can be found as:

$$\dot{E}x_F = \dot{E}x_P + \sum_k \dot{E}x_{D,k} + \dot{E}x_L \tag{3}$$

and more explicitly;

$$\sum \left(1 - \frac{T_0}{T_k}\right) \dot{Q}_k - \dot{W} + \sum \dot{m}_{in} \psi_{in} - \sum \dot{m}_{out} \psi_{out} = \dot{E}x_D \tag{4}$$

where $\dot{E}x_F$, $\dot{E}x_P$, $\dot{E}x_D$ and $\dot{E}x_L$ are the exergy rates associated with the fuel, product, exergy destruction and exergy loss of the overall system, respectively. $\dot{Q}_k$ is the heat transfer rate crossing the boundary at temperature T_k at location *k*, $\dot{W}$ is the work rate, the subscript zero indicates properties at the restricted dead state of P_0 and T_0, and ψ is the specific flow exergy as given below:

$$\psi = (h - h_0) - T_0(s - s_0) \tag{5}$$

where h_0 and s_0 denote the enthalpy and entropy in the reference case, respectively.

If the system boundaries are assumed in the reference state of T_0, the exergy losses related to the kth component are not mentioned [9]. Exergy losses appear only at the level of the overall system. In this situation the exergy balance at the component level may be simplified as:

$$\sum_k \dot{E}x_{D,k} = \dot{E}x_{F,k} - \dot{E}x_{P,k} \tag{6}$$

Finally the basic assumptions used in thermodynamic modelling may be given as: (i) all processes occur within steady state and stable volume conditions, (ii) differences in kinetic and potential energy are neglected, (iii) heat loss occurring in components and pressure drops within valves and pipes are not considered, (iv) the thermodynamic properties of water are used for the geofluid (brine), (v) the air is assumed to be an ideal gas with homogenous distribution in air-cooled condensers and (vi) the isentropic efficiencies of the turbines, pumps and fans are used, (vii) the direct drive balancing between the generator and the turbines is ignored by opening the injection valves on the turbine, (viii) the geofluid temperature for re-injection does not fall below 80 °C and (ix) the limit value ($\geq$0.98 for $x_{12,13,19,20}$) of the quality of steam to prevent excessive damage to the turbine blades is accepted.

2.3. Analysis and optimization processes for the system

To gain a better understanding of a problem, the following terms should be defined that analysis is the process of breaking a complex topic or substance into smaller parts [31] while optimization is the process of finding an alternative with the most cost effective or highest achievable performance under the given constraints, by maximizing desired factors and minimizing undesired ones [32]. Finally, there are two different solution routes to better understand and resolve a problem in both processes. The analysis and optimization methods used in this study are conventional and advanced exergy analyses and artificial bee colony (ABC) optimization method. The problem addressed in this study is a rather complex and non-linear problem, so it is difficult to solve it with mathematical methods as No Free Lunch theorem [33]. They do not demonstrate same performance when the domain and/or the structure problem can be changed [34]. Therefore, our problem can be solved with heuristic methods. Among the best known heuristic optimization methods like GA, PSO and DE, the reason for choosing the ABC optimization method is that it is the most effective and advantageous for multivariate problems [22,23,35,36].

2.3.1. Advanced exergy analysis

The advanced exergy analysis is administered to evaluate the mutual interdependencies among the system components and the realistic potential for improving the components. However, such an evaluation can not be done with the conventional exergy analysis [9]. Its methodology has been discussed in more detail in Refs. [37–45].

In the analysis, the interactions among system components can be evaluated by splitting into endogenous (EN) and exogenous (EX) portions of the exergy destruction rate within the kth component [46], which is given by

$$\dot{E}x_{D,k} = \dot{E}x_{D,k}^{EN} + \dot{E}x_{D,k}^{EX} \tag{7}$$

where the endogenous portion, $\dot{E}x_{D,k}^{EN}$, is the exergy destruction rate of the kth component related to itself. The calculation of $\dot{E}x_{D,k}^{EN}$ can be done in case that the kth component works under the real conditions while the remaining components work under theoretical conditions. The other portion, $\dot{E}x_{D,k}^{EX}$, is the exergy destruction rate caused by the remaining components. It may be found by subtracting the endogenous exergy destruction rate from the real exergy destruction.

To evaluate the real potential for improving the components, their exergy destruction rates are split into unavoidable (UN) and avoidable (AV) parts [47,48], as follow

$$\dot{E}x_{D,k} = \dot{E}x_{D,k}^{UN} + \dot{E}x_{D,k}^{AV} \tag{8}$$

where the unavoidable portion, $\dot{E}x_{D,k}^{UN}$, is the exergy destruction rate not to be recovered due to technological limitations. The calculation is made assuming the most appropriate operating conditions by considering each component as isolated from the system. The assumptions for the unavoidable conditions simulation are linked to the decision maker and may be arbitrary to a degree [41,47,48]. It may be given as below [49,50]:

$$\dot{E}x_{D,k}^{UN} = \dot{E}x_{P,k}\left(\frac{\dot{E}x_D}{\dot{E}x_P}\right)_k^{UN} \tag{9}$$

The exergy destruction given above may be divided into separated portions again to create new parameters to ensure better understanding of the interaction between components and the improvement potentials [51]. The unavoidable endogenous, $\dot{E}x_{D,k}^{UN,EN}$, unavoidable exogenous, $\dot{E}_{D,k}^{UN,EX}$, avoidable endogenous, $\dot{E}x_{D,k}^{AV,EN}$, and avoidable exogenous, $\dot{E}x_{D,k}^{AV,EX}$, exergy destruction rates are calculated, respectively, using [49–52].

$$\dot{E}x_{D,k}^{UN,EN} = \dot{E}x_{P,k}^{EN}\left(\frac{\dot{E}x_D}{\dot{E}x_P}\right)_k^{UN} \tag{10}$$

$$\dot{E}x_{D,k}^{UN,EX} = \dot{E}x_{D,k}^{UN} - \dot{E}x_{D,k}^{UN,EN} \tag{11}$$

$$\dot{E}x_{D,k}^{AV,EN} = \dot{E}x_{D,k}^{EN} - \dot{E}x_{D,k}^{UN,EN} \tag{12}$$

$$\dot{E}x_{D,k}^{AV,EX} = \dot{E}x_{D,k}^{EX} - \dot{E}x_{D,k}^{UN,EX} \tag{13}$$

2.3.2. Artificial bee colony (ABC) optimization method

Karaboğa [35,36] developed the artificial bee colony (ABC) algorithm by modelling the food search behaviour of bees. Among the intelligent nutrition behaviour of honey bees are finding rich food sources near the hive, dancing to direct other bees to a hive or rich sources and abandoning consumed sources to find potentially richer sources of nectar [53]. The ABC optimization algorithm attempts to find the location of the richest source of nectar by iteratively finding points providing minimum or maximum solutions to the problem in space. Among the known heuristic optimization methods like GA, PSO and DE, the ABC algorithm has major benefits in multi-objective function problems. ABC algorithm has fewer constraints while it considers a limiting parameter to increase the convergence speed of optimization. Premature convergence problem occurs less in ABC than in GA and PSO algorithms [22,23,35,36]. ABC algorithm produces new solutions by a simple operation and diversification of the solutions is controlled by random selection. This accelerates the foraging procedure and the convergence to an optimum value. Solutions with higher fitness values are selected which leads to a quick and detailed search over search space on each cycle of optimization. Owing to the selection schemes randomly employed and the neighbour generation mechanism applied, ABC has better performance in terms of local and the global optimization [22,23]. ABC algorithm are its better or at least similar function to that of optimization algorithms, although it has less control parameters making ABC algorithm more efficient in optimizing multi-modal and multi-dimensional problems [22,23,35]. The process involved in this model comprises the following steps [36,54–56]:

- At the beginning of the food search process, explorer bees randomly begin to search for food.
- After finding a food source, explorer bees become duty bees and begin to carry nectar from the source to the hive. Each d2uty bee empties nectar brought to the hive and at this point either returns to the source found earlier or communicates information related to the source to observer bees in the hive by dancing in the dance area. If the source has been consumed, the duty bee becomes an explorer bee and begins to search for new sources.
- The observer bees waiting in the hive watch the dances indicating rich sources and choose a source linked to the dance frequency which is proportional to the quality of the food.

The ABC algorithm firstly produces random values between the upper and lower limits for each parameter in a random location production process as seen in Eq. (14).

$$x_{ij} = x_j^{\min} + rand(0,1)\left(x_j^{\max} - x_j^{\min}\right) \quad \begin{cases} i = 1,\ldots,SN \\ j = 1,\ldots,D \end{cases} \tag{14}$$

where SN is the number of food sources (or employed bees) and D is the number of parameters to be optimized.

After the initial stage, the food sources pass through duty bee, observer bee and explorer bee processes in an attempt to find the best source. The maximum cycle number (MCN), acceptable error value or other stopping criteria may be used as stopping criteria for the ABC algorithm. In this optimization process the number of food sources is equal to the number of duty bees. Worker bees determine new food adjacent to the working food source and assess its quality. If the new source is better than the first, the new source is remembered. The determination of a new source adjacent to the current source is given in:

$$v_{ij} = x_{ij} + \phi_{ij}\left(x_{ij} - x_{kj}\right) \qquad \begin{cases} j = 1,2,\ldots,SN \\ k = 1,2,\ldots,SN \end{cases} \tag{15}$$

where φ is random number in range of [-1,1] and $j \neq k$. As the difference between the random values of x_{ij} and x_{kj} reduces, in other words as solutions become similar, the change amount for the x_{ij} parameter reduces. Thus, as the regional optimal solution becomes closer, the change amount adaptively reduces.

The v_i parameter vector produced within limits represents a new source and its quality is obtained by calculating the fitness value (fit) given by

$$fit_i \quad \begin{cases} \dfrac{1}{1+f_i}, & f_i \geq 0 \\ 1 + |f_i|, & f_i < 0 \end{cases} \tag{16}$$

where f_i is the cost values of solving the v_i source.

Depending on the nectar amount between x_i and v_i, namely the fit value, a greedy selection process is applied [57]. If the newly found v_i solution is better, the duty bee wipes the old source from memory and replaces it with the location of v_i. If this is not the case, the duty bee continues to go to x_i source and as the x_i solution could not be developed, the non-development counter related to this source increases. If the solution is developed the counter goes to zero.

After all duty bees have completed research in a cycle, they return to the hive and communicate information related to the nectar amounts in the sources found to observer bees. Each observer bee benefits from information shared through dancing and chooses a region (source) proportional to the amount of nectar in the food source [58]. In this basic ABC algorithm the selection process linked to the fit value is completed using a roulette wheel [57]. The angle of each section of the wheel is proportional to a fit value as:

$$p_i = \frac{fit_i}{\sum_{i=1}^{SN} fit_i} \tag{17}$$

Depending on the calculation of this probability, as the amount of nectar in a source increases (as the fit value increases), the number of observer bees choosing this source region will increase. This property shows that the ABC has similar behaviour to the positive feedback property of the behaviour of natural bees.

After calculating the probability values of the algorithm, these values are used according to the roulette wheel selection process to produce random numbers in the interval [0 1] for each source and if the p_i value is larger than this produced number, the duty bee uses Eq. (15) to produce a new solution in the source region, like the observer bee. The new solution is assessed and quality is calculated. Later the fit of the new solution is compared to the old solution and the best is chosen by using the greedy selection process. If the new solution is better, this solution is taken in place of the old solution and the non-development counter is set to zero. If the fit of the old solution is better, this solution is protected and the non-development counter increases. This process continues until all observer bees have been released to a food source location [59].

2.3.3. Objective function

The analysis and optimization processes produce many possible solutions to some problems. However, a function should be chosen to find the correct and acceptable solution and to compare with alternative solutions. In the literature this function is called the objective function. Therefore, only by choosing a target function for the evaluation and optimization of a thermodynamic system can it be analysed and optimized. The single objective function in this study is determined as the exergy efficiency (ε_{sys}) of the whole system. In the thermodynamic evaluation, the exergy efficiency [60–62] for the conventional exergy analysis (CExA), the modified exergy efficiency [49–52] for the advanced exergy analysis (AExA), and the maximum possible exergy efficiency by using the artificial bee colony (ABC) method can be defined (in system and component levels), respectively as

$$\varepsilon_{sys} = \frac{\dot{E}x_{P,sys}}{\dot{E}x_{F,sys}} = 1 - \frac{\dot{E}x_{D,sys}}{\dot{E}x_{F,sys}} \tag{18a}$$

$$\varepsilon_k = \frac{\dot{E}x_{P,k}}{\dot{E}x_{F,k}} = 1 - \frac{\dot{E}x_{D,k}}{\dot{E}x_{F,k}} \tag{18b}$$

$$\varepsilon_{modified,sys} = \frac{\dot{E}x_{P,sys}}{\dot{E}x_{F,sys} - \dot{E}x^{UN}_{D,sys} - \dot{E}x^{AV,EX}_{D,sys}} \tag{19a}$$

$$\varepsilon_{modified,k} = \frac{\dot{E}x_{P,k}}{\dot{E}x_{F,k} - \dot{E}x^{UN}_{D,k} - \dot{E}x^{AV,EX}_{D,k}} \tag{19b}$$

$$\varepsilon_{\max\ possible,sys} = \frac{\dot{E}x_{P,sys,\max}}{\dot{E}x_{F,sys}} = 1 - \frac{\dot{E}x_{D,sys,\min}}{\dot{E}x_{F,sys}} \tag{20a}$$

$$\varepsilon_{\max\ possible,k} = \frac{\dot{E}x_{P,k,\max}}{\dot{E}x_{F,k}} = 1 - \frac{\dot{E}x_{D,k,\min}}{\dot{E}x_{F,k}} \tag{20b}$$

where $\varepsilon_{\max\ possible\ sys}$ is that variables that maximize the exergy efficiency (ε_{sys}) of the whole system and their limits are found as a result of the optimization process performed.

3. Results and discussion

In this study, the analysis and optimization methods are used to assess the performance in terms of thermodynamics of a binary geothermal power plant (GPP) to (i) improve the thermodynamic performance of the system and its components and (ii) compare the results of the analysis (exergy) and optimization (artificial bee colony) methods about system performance. The Sinem GPP operated in Turkey as a case study is chosen. With this aim, the temperature, pressure and mass flow rate for each state within the system are collected on the 14 April 2013 as shown in Fig. 1. The procedure mentioned in the thermodynamic modelling section is performed with the MATLAB program associated with the COOLPROP to obtain the results in Table 1. Before applying the advanced exergy analysis and artificial bee colony optimization method to the available system, the necessity to complete conventional exergy analysis is not forgotten because this is provided the target function of the study.

Table 2
The exergetic variables for the GPP system and all its components.

Component, *k*	$\dot{E}x_{F,k}$ (kW)	$\dot{E}x_{P,k}$ (kW)	$\dot{E}x_{D,k}$ (kW)	$\dot{E}x_{L,tot}$ (kW)
CON 1	6069.49	4094.42	1975.06	–
CON 2	5553.70	3062.96	2490.75	–
PRE-HE 1	4273.64	3634.71	638.93	–
PRE-HE 2	5678.41	4586.55	1091.86	–
TURB 1	12908.34	12066.15	842.19	–
TURB 2	10801.98	9000.32	1801.65	–
VAP 1	16682.38	15365.76	1316.61	–
VAP 2	13950.34	11494.18	2456.16	–
RECUP	1041.22	621.05	420.17	–
PU 1	2323.60	397.53	1926.04	–
PU 2	2192.20	274.95	1917.26	–
Overall system	53771.73	21028.56	16876.69	15866.48

3.1. Results of the conventional exergy analysis (CExA)

Using the data in Table 1 and Eq. (3) or (4), the thermodynamic analysis (conventional one) for the Sinem GPP and its components is performed. The results obtained from applying the conventional exergy analysis (CExA) are given in Table 2. As seen in Table 2 there is an exergy input of 53772 kW to the system from the geothermal fluid. Of this total exergy input, nearly 15866 kW is calculated to be exergy loss due to re-injection and NCG. As a result, while the exergy destruction rate occurring from all components in the system is 16876 kW, the exergy amount produced by the system is

Table 1
The recorded and calculated thermodynamics variables at various system locations for the Sinem GPP on 14.04.2013.

Steam, j	Fluid type	T_j (°C)	P_j (kPa)	h_j (kJ/kg K)	s_j (kJ/kg K)	$\dot{m}_j$ (kg/s)	$\dot{E}x_j$ (kW)
1	Brine	164	1040	692.43	1.98	445	52693
1′	Brine - steam	165	1040	696.78	1.99	5.83	699
1′	NCG	165	1040	629.69	2.64	2.50	380
2	Brine	136	730	573.07	1.70	445	36010
3	Brine	110	690	459.30	1.41	445	22589
4	Brine	110	690	459.30	1.41	222.50	11295
5	Brine	110	690	459.30	1.41	222.50	11295
6	Brine	89	590	371.51	1.18	222.50	7021
7	Brine	81	570	337.74	1.08	222.50	5616
8	Brine	85	590	354.54	1.13	445	12447
9	Brine	107	690	448.50	1.38	0.83	40
10	Brine - steam	107	690	448.50	1.38	5.25	253
10	NCG	107	690	575.29	2.58	2.25	257
11	*n*-pentane	105	1261	176.25	0.51	160	4776
12	*n*-pentane	137	1261	516.04	1.35	160	20142
13	*n*-pentane	82	150	440.76	1.36	160	7237
14	*n*-pentane	60	150	398.48	1.24	160	6193
15	*n*-pentane	31	150	−11.44	−0.04	160	123
16	*n*-pentane	37	1261	3.07	0.00	160	520
17	*n*-pentane	55	1261	47.00	0.14	160	1141
18	*n*-pentane	106	687	179.16	0.52	169	5018
19	*n*-pentane	109	687	469.92	1.28	169	16512
20	*n*-pentane	69	119	416.78	1.32	169	5713
21	*n*-pentane	33	119	−7.00	−0.02	169	157
22	*n*-pentane	39	687	5.93	0.02	169	431
23	Air	25	101	424.29	3.88	2000	0
24	Air	25.5	106	424.70	3.87	2000	8238
25	Air	25	101	424.29	3.88	2000	0
26	Air	25.5	106	424.70	3.87	2000	8238

Note: The environmental temperature and pressure on that date were recorded as 25 °C and 1 bar, respectively.

21029 kW. The highest exergy destruction rate in the power plant is nearly 2491 kW occurring in the condenser CON 2. This is followed by the vaporizer VAP 2 and the condenser CON 1. In this situation it is understood that the components requiring priority improvement are CON 2, VAP 2 and CON 1, respectively. However, the cause of the exergy destruction is not sufficient to allow us to understand what the interaction between the components is and how to complete the improvements. Additionally, our objective function of total exergy efficiency is found to be 39.11% based on the exergy input from the geofluid (brine) entering the GPP according to the CExA.

3.2. Results of the advanced exergy analysis (AExA)

Advanced exergy analysis (AExA) is an analysis type focusing not on the system as a whole, but on the component level; in other words, only on the exergy destruction amounts in components. It is used to assess the thermodynamic performance of the Sinem GPP comprising 11 pieces of components. Using the unavoidable and theoretical operating conditions given in Table 3, the exergy destruction rate of the 11 components of the GPP system are divided into endogenous/exogenous and unavoidable/avoidable portions. Thus, reduction of the exergy destruction of the system components will be divided into resources (endogenous/exogenous sections) and potential (unavoidable/avoidable sections). The algorithm written in the MATLAB program associated with the COOLPROP is used to simulate the Sinem GPP based on a plant model that uses actual and variable data.

To calculate the endogenous exergy destruction rates for system components, the real and theoretical operating conditions in Tables 1 and 3 are used. The calculation procedure involved all equipment in the system working under theoretical conditions while the calculated component was working under real operating conditions. During this process, the output power of the whole system was held constant [63]. It should be noted that theoretical operating conditions are impossible with real world engineering. The exogenous exergy destruction rate for the component used is calculated using Eq. (7). The AExA results completed to find whether the amount of exergy destruction in components of the Sinem GPP was due to the component or to neighbouring components are listed in the second and third columns of Table 4.

Table 3
The unavoidable and theoretical operation conditions conducted for the study.

Component, k	Parameter	Unavoidable conditions	Theoretical conditions
CON 1	ΔT_{pinch}	3 K	0 K
	ΔP	10 kPa	0 kPa
CON 2	ΔT_{pinch}	3 K	0 K
	ΔP	10 kPa	0 kPa
PRE-HE 1	ΔT_{pinch}	43 K	0 K
	ΔP	10 kPa	0 kPa
PRE-HE 2	ΔT_{pinch}	5 K	0 K
	ΔP	10 kPa	0 kPa
TURB 1	η_{is}	93%	100%
	η_{mech}	100%	100%
TURB 2	η_{is}	93%	100%
	η_{mech}	100%	100%
VAP 1	ΔT_{pinch}	6 K	0 K
	ΔP	10 kPa	0 kPa
VAP 2	ΔT_{pinch}	5 K	0 K
	ΔP	10 kPa	0 kPa
RECUP	ΔT_{pinch}	5 K	0 K
	ΔP	10 kPa	0 kPa
PU 1	η_{is}	82%	100%
	η_{mech}	100%	100%
PU 2	η_{is}	77%	100%
	η_{mech}	100%	100%

On Table 4, the majority of exergy destruction rate of all components apart from the pumps are endogenous, that is, sourced within the components themselves. The difference in endogenous and exogenous exergy destruction rates specially in CON 2, VAP 2 and CON 1 is very large. The choice of low capacity condensers at the start and then the polluting and dampening effect of the cooling water within them reduce the efficiency of the condensers. Due to these reasons, higher levels of endogenous exergy destruction rate occur. This situation affects PU 1 and PU 2 more as they have pressure falls due to the pollution and dampening within the condensers. As a result, their exogenous exergy destruction is greater than the endogenous one. In the situation where there output temperature of turbine TURB 2 and the cooling water input temperature falls, CON 2 is affected exogenously. Low turbine yield for TURB 1 is due to temperature differences, leaks and pressure drops, in other words due to itself, with very high exergy destruction rate of 1244 kW. The endogenous exergy destruction rate is nearly 558 kW. This is caused by temperature drops occurring at the output of the vaporizer VAP 2. In the second level, the same reasons can be mentioned for TURB 1. The VAP 2 system component has higher exergy destruction rate than VAP 1 in the first level. The reason for this is due to the great fall in geofluid temperature coming out of VAP 1. If this output temperature were increased, this would increase the exergy destruction rate of VAP 1. Therefore, exogenous exergy destruction rate caused by VAP 1 would occur in VAP 2. If there was improvement within the vaporizer VAP 1 in the system, this would cause a reduction in the exogenous exergy destruction rate in the turbine TURB 1. Additionally, reducing the exogenous exergy destruction rate in VAP 2 would thus cause a reduction in the exogenous exergy destruction rate in TURB 2.

To calculate the unavoidable exergy destruction rate in system components, the unavoidable operating conditions (best possible working conditions) in Table 4 are used. Thus when all components in the system is operated under unavoidable conditions, the exergy destruction occurring in the calculated component is the unavoidable exergy destruction rate. Determination of unavoidable operating conditions is completely linked to the decision maker and it should be noted are arbitrary to a degree. Additionally, the avoidable exergy destruction rate can be easily calculated using Eq. (8). In conclusion, the results of the AExA analysis performed to determine whether there is improvement potential for the exergy destruction in system components or to understand how this may occur, are listed in the fourth and fifth columns in Table 4.

In Table 4, the avoidable exergy destruction rate is higher than the unavoidable exergy destruction rate for all components, apart from components like TURB 1, TURB 2, VAP 2, RECUP, PU 1 and PU 2. The main components producing power in the system of TURB 1 and TURB 2 have very high unavoidable exergy destruction. This means that these turbines need maintenance or to be replaced. Within these components it is understood there is only 43 kW and 563 kW improvement potential. Among the components CON 2 has highest value for avoidable energy destruction of 1929 kW. This means that this component has very high improvement potential. This is followed by the components CON 1 and VAP 1 with values of 1443 and 1095 kW, respectively.

For more advanced analyses, the endogenous and exogenous portions of the unavoidable and avoidable exergy destruction rates in the components may be determined. The results obtained using Eqs. (10)–(13) are presented in Table 4. The most significant portion of the AExA analysis is the avoidable endogenous portion and this portion should be specially evaluated. In Table 4, it appears that endogenous exergy destruction rate may be prevented in all components apart from the pumps. This destruction in the pumps is due to the temperature of the *n*-pentane emerging from the

Table 4
The advanced exergetic variables for the GPP system and all its components.

Component, *k*	$\dot{E}x^{EN}_{D,k}$(kW)	$\dot{E}x^{EX}_{D,k}$(kW)	$\dot{E}x^{AV}_{D,k}$(kW)	$\dot{E}x^{UN}_{D,k}$(kW)	$\dot{E}x^{UN}_{D,k}$		$\dot{E}x^{AV}_{D,k}$	
					$\dot{E}x^{UN,EN}_{D,k}$(kW)	$\dot{E}x^{UN,EX}_{D,k}$(kW)	$\dot{E}x^{AV,EN}_{D,k}$(kW)	$\dot{E}x^{AV,EX}_{D,k}$(kW)
CON 1	1551.15	423.91	1442.77	532.29	122.75	409.54	1428.40	14.37
CON 2	1647.90	842.85	1928.88	561.87	109.20	452.66	1538.69	390.19
PRE-HE 1	353.34	285.59	359.98	278.95	102.94	176.01	250.40	109.58
PRE-HE 2	576.79	515.07	641.86	450.00	167.56	282.44	394.81	247.05
TURB 1	692.86	149.33	43.32	798.87	657.17	141.70	35.70	7.63
TURB 2	1243.81	557.84	563.16	1238.49	855.01	383.49	388.80	174.35
VAP 1	844.42	472.19	1095.44	221.17	141.43	79.75	703.01	392.42
VAP 2	1614.73	841.43	708.13	1748.03	940.63	807.40	674.10	34.03
RECUP	224.25	195.92	68.06	352.11	256.96	95.15	52.37	15.69
PU 1	757.58	1168.46	309.51	1616.53	609.72	1006.81	147.86	161.65
PU 2	457.05	1460.21	460.83	1456.43	316.05	1140.38	141.00	319.83
Overall System	12105.42	4772.09	7585.91	9291.60	6929.24	2362.39	5176.21	2409.73

condensers. Among system components CON 2 has the highest avoidable endogenous exergy destruction rate. This is followed by CON 1 and VAP 1. In conclusion, when the components with highest improvement potential are listed they are found during CON 2, CON 1 and VAP 2. However, in the CExA this order was CON 2, VAP 2 and CON 1.

3.3. Results of the artificial bee colony (ABC)

The previously mentioned artificial bee colony (ABC) was used to optimize the value of the total exergy efficiency in the system (to maximize its value). The converging conditions and their values used in ABC are given in Table 5. As seen in the table, there is one parameter to be optimized and this is the single objective function (as total exergy efficiency of the system). The 9 decision variables and their constraints used in the ABC algorithm to find the maximum possible exergy efficiency are presented in Table 6. It should not be forgotten that there are at least 78 decision variables at 26 points within the GPP system considered. To optimize such a large number of variables, the computer operation time is endless. As a result, the decision variables in Table 6 were very carefully chosen. They are the most important variables that affect the system performance and efficiency. Constraints should be determined accordingly to resolve any thermodynamic problem. In this study, they consist of the pressure and mass flow rate values of the components on the line through which the geothermal fluid passes. By using the decision variables and their constraint range, the ABC algorithm is used to optimize total exergy efficiency of the Sinem GPP model on which the algorithm is written in the MATLAB program associated with the COOLPROP. Each optimization procedure was repeated at least once to obtain appropriate results.

The convergence behaviour of the ABC algorithm to optimize the thermodynamic performance of the Sinem GPP is given in Fig. 2. As seen in Fig. 2, the exergy efficiency is maximised on the 4th cycle. Though there is a slow drop until the 27th cycle, maximum exergy efficiency converges at nearly the 28th food search cycle. As can be seen, the maximum exergy efficiency was found to be 42.80%.

Table 7 presents the true and optimum values of the decision variables chosen during optimization of the system. As listed in Table 7, the true and optimum values for the input pressure of the geofluid into the system are respectively 1040 kPa and 1107.7 kPa. For geofluid steam these values are calculated as 1040 kPa and 1095.3 kPa, respectively. As can be seen, the optimum values are higher than the true values. Similar results are obtained for their mass flow rates. Additionally, the pressure differences between the input and output geofluid in vaporizers and preheaters should be lowered. If possible, it is necessary to lower the percentage of NCG.

Table 5
The converging conditions used in the ABC algorithm.

Parameters	Value
Number of colony size (NP)	10
Number of food sources	10
Number of colony cycles	50
Boundary (limit and max cycle)	100
Number of parameters for optimization process (D)	1
Iterative relative convergence error tolerance, %	0.05

Table 6
The decision variables and their constraints determined for the ABC method (only geofluid/brine line of the GPP).

Decision variables	Unit	Constraint range (to … from …)
P_1	kPa	950–1150
$P_{1,steam}$	kPa	950–1150
$\Delta P_{VAP\ 1}$	kPa	0–440
$\Delta P_{VAP\ 2}$	kPa	0–230
$\Delta P_{PRE\text{-}HE\ 1}$	kPa	0–200
$\Delta P_{PRE\text{-}HE\ 2}$	kPa	0–200
$\dot{m}_1$	kg/s	442–446
$\dot{m}_{1,steam}$	kg/s	8–10
NCG	%	20–40

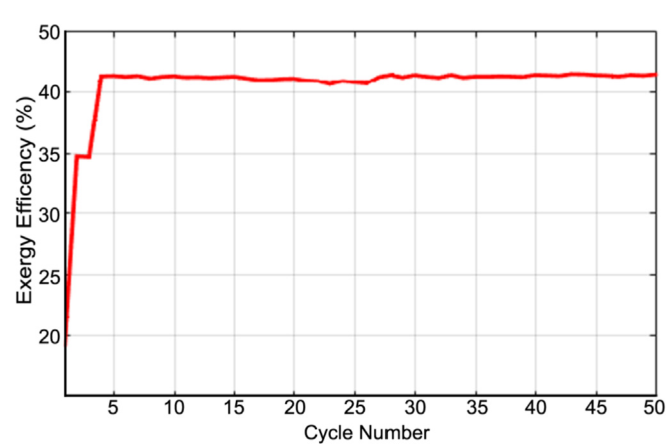

Fig. 2. The convergence behaviour of ABC algorithm for maximizing exergy efficiency of whole system.

Table 7
The real and optimized values of the decision variables for the GPP system.

Decision variables	Real value	Optimum value
P_1	1040	1107.70
$P_{1,steam}$	1040	1095.30
$\Delta P_{VAP\ 1}$	310	123.26
$\Delta P_{VAP\ 2}$	40	10.34
$\Delta P_{PRE\text{-}HE\ 1}$	100	84.85
$\Delta P_{PRE\text{-}HE\ 2}$	120	59.35
$\dot{m}_1$	445	446
$\dot{m}_{1,steam}$	8.33	9.32
NCG	30	27

Table 8
The maximum possible exergetic variables obtained from the ABC method for the GPP system and all its components.

Component, *k*	$\dot{E}x_{F,k}$ (kW)	$\dot{E}x_{P,k}$ (kW)	$\dot{E}x_{D,k}$ (kW)	$\dot{E}x_{L,tot}$ (kW)
CON 1	5983.26	4108.19	1875.07	–
CON 2	5554.04	3163.29	2390.75	–
PRE-HE 1	4488.51	3845.92	642.59	–
PRE-HE 2	5733.43	4713.45	1019.98	–
TURB 1	12904.32	12166.15	738.17	–
TURB 2	10801.59	9100.32	1701.27	–
VAP 1	16630.73	15487.45	1143.28	–
VAP 2	13997.43	11594.18	2403.25	–
RECUP	1145.20	700.60	444.60	–
PU 1	2224.84	398.8	1826.04	–
PU 2	2165.26	348.01	1817.25	–
Overall system	54044.93	23130.24	16002.25	14639.24

In conclusion, if the optimum values for the decision variables can be reached, the total system exergy efficiency will reach maximum.

The maximum possible exergetic variables obtained with the ABC method are listed in Table 8. In Table 8 there is nearly 54045 kW exergy input into the GPP system. Of this total exergy input nearly 4639 kW is exergy loss due to both re-injection and NCG. The exergy destruction rate caused by whole system components is 16002 kW, while the exergy rate produced by the system is 23130 kW. The highest exergy destruction rate in the GPP is 2403 kW occurring in the vaporizer VAP 2. This is followed by the condensers CON 2 and CON 1. In this situation the components requiring priority improvement are understood to be VAP 2, CON 2 and CON 1.

3.4. Comparison of the methods conducted for the system performance

Fig. 3 shows the variation in exergy destruction rates for the system components at the three methods. Regarding Fig. 3, similar to the AExA analysis results, the ABC method optimizes decision variables chosen along the geothermal fluid line according to accepted constraints to reduce the exergy destruction rates of all components. As seen in Fig. 3, the component with highest exergy destruction is the condenser CON 2. However, according to the ABC method, it is the vaporizer VAP 2. From a different aspect, condenser CON 2 had exergy destruction rates of 2491 kW and 2403 kW according to the CExA and the ABC, respectively. According to the AExA analysis, this value was 1539 kW. When these methods are compared, a very low exergy destruction rate was obtained from the AExA analysis. This is a reality of the assumptions in the AExA analysis being linked to the decision maker and arbitrary to an extent [41,47,48]. In this situation, this means that to complete the AExA analysis accurately requires experience and ability.

The unavoidable portion of the exergy destruction rates in system components is obtained by subtracting separately the exergy destruction rates obtained in the other two methods from the exergy destruction rates in the CExA. Thus, these last two methods can be compared more clearly. The obtained results are presented in Fig. 4. As seen on Fig. 4, the unavoidable portion of the exergy destruction amounts for component in the ABC method is much lower than in the AExA analysis. For example, for the condenser CON 2 the value is 562 kW for the AExA and 100 kW for the ABC. Additionally, on AExA analysis the unavoidable portions for the vaporizer VAP 2, pumps PU 1 and PU 2 and turbine TURB 2 are 1748 kW, 1617 kW, 1456 kW and 1238 kW, respectively, while for ABC analysis these values are 53 kW, 100 kW, 100 kW and 101 kW, respectively. Thus, the largest difference between the two methods is due to the vaporizer VAP 2.

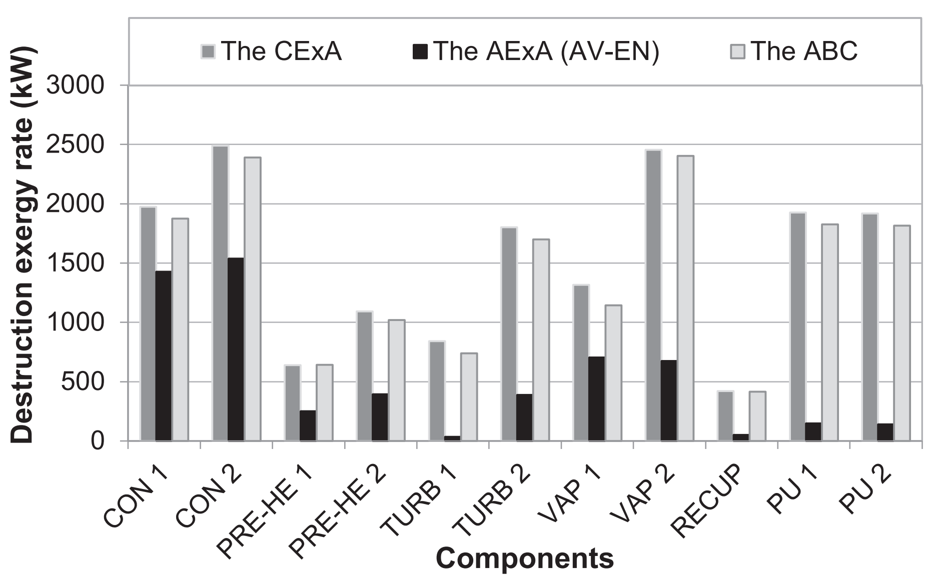

Fig. 3. The change of destruction exergy rates of the system components for the conventional and advanced exergy analyses (CExA and AExA) and the artificial bee colony (ABC) method.

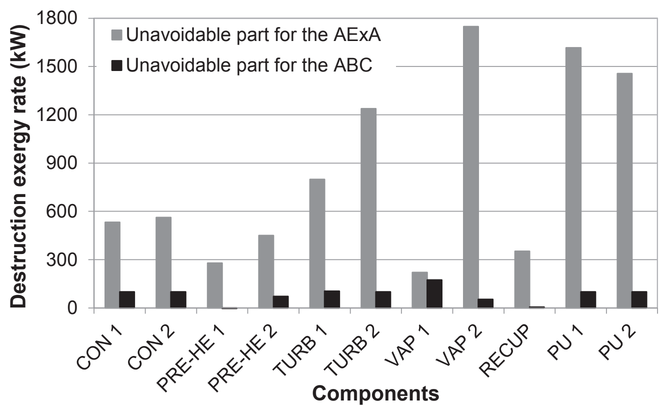

Fig. 4. The change of unavoidable destruction exergy rates for the system components in the AExA and ABC methods.

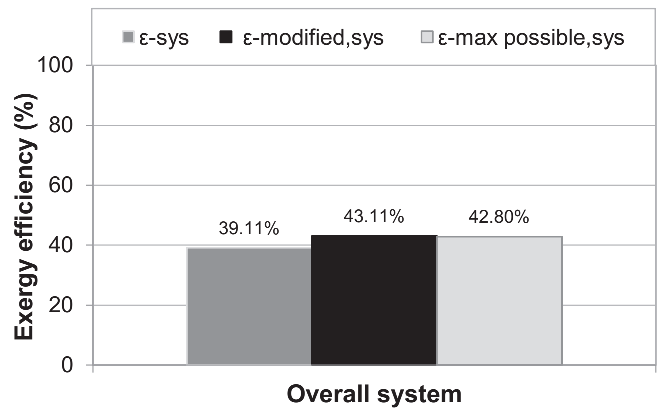

Fig. 6. The comparison of exergy efficiencies for overall system in the three different methods.

A comparison of the exergy efficiencies at the component level obtained from the three different methods used in the study is given in Fig. 5. In this way it can be observed which methods are more significant. As seen in Fig. 5, for the exergy efficiency values for all components it is appeared that exergy efficiency on the AExA analysis is higher than those from the other two methods. This indicates that if the maximum improvement to the component within the system is completed, its efficiency will only reach as high as the modified exergy efficiency (of the AExA). However, while the maximum possible exergy efficiency with the ABC method is higher than that of the CExA analysis, it is lower than that of the AExA analysis. The reason for this may be that assumptions are linked to the decision maker and somewhat arbitrary. From Fig. 5, the real exergy efficiencies (CExA) for TURB 1 and TURB 2 were 93.5% and 83%, respectively while if the maximum improvements were made the modified exergy yields (AExA) would only be 99.7% and 95.9%. On the other hand, with the ABC method their maximum possible exergy efficiencies are 94.3% and 84.2%, respectively. As seen in the figure, the CExA and ABC methods have lowest values of exergy efficiencies for the pumps, while according to the AExA analysis, the efficiencies are seen to rise to nearly 70%.

Fig. 6 shows a comparison of the methods considering exergy efficiency of the whole system. Regarding Fig. 6, under real conditions in the system the total system efficiency from the CExA is found to be 39.11%, while with maximum improvements performed the exergy efficiency will increase to 43.11%. When the system is optimized according to the ABC method, the maximum possible exergy efficiency will only reach 42.80%. The AExA and ABC methods produce very close results for total exergy efficiency of the system.

It is thought that as temperatures, mass flow rates and pressures are measured, total uncertainties for all these parameters are individually determined using the method described by Holman [64]. In the present study, total uncertainties for the measured parameters such as temperature, pressure and volumetric flow rate are 1.05% (in °C), 1.98% (in kPa) and 2.37% (in m^3/s), while the total uncertainties for the calculated parameters such as exergy input rate, exergy output rate, exergy efficiency, modified exergy efficiency and maximum possible exergy efficiency are 1.02% (in kW), 1.41% (in kW), 2.14%, 6.34% and 2.51%, respectively.

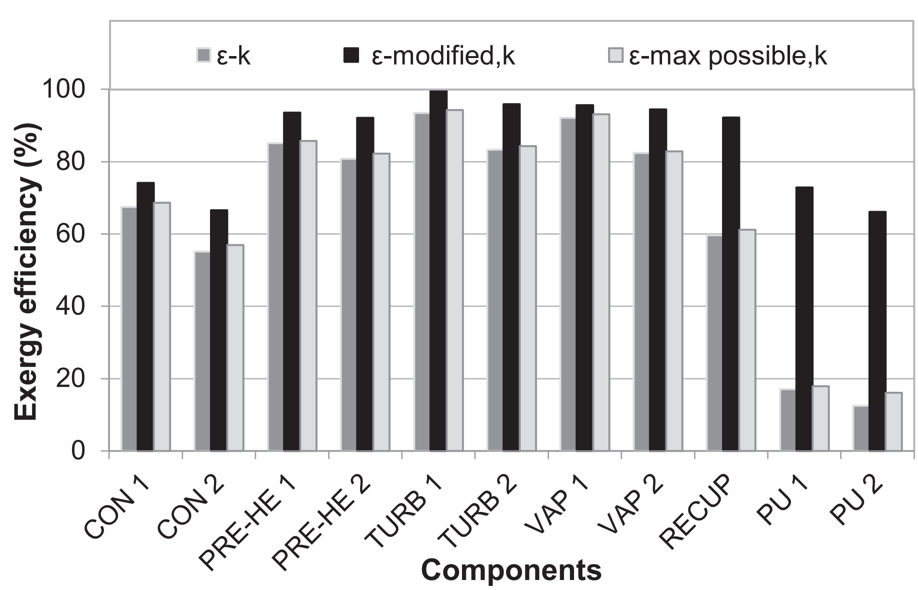

Fig. 5. The comparison of exergy efficiencies for the system components in the three different methods examined in this study.

4. Conclusions

In this study, the conventional (CExA) and advanced (AExA) exergy analyses in addition to the optimization method of the artificial bee colony (ABC) are applied to an available operating geothermal binary power plant (Sinem GPP in Turkey) to improve the thermodynamic performance of the system. Initially a simulation model accurately representing the real system is created. Then the conventional and advanced exergy analyses are considered on the model. Finally, to maximize total exergy efficiency in the system, the optimization procedure using the ABC method is performed on the system model. As mentioned above the results obtained from the three methods are compared to assess thermodynamic performance of whole system. Thus, the study impels us to the results listed below:

a) The total exergy efficiency of the system is found to be 39.1%, 43.1% and 42.8%, respectively, for the CExA, AExA and ABC methods. The exergy efficiencies in the AExA and ABC methods are observed to be very close.
b) The exergy rate produced in Sinem GPP is 21028 kW according to the CExA and AExA analyses, while this value reaches 23130 kW for the ABC method. In this situation the difference in these values of 2102 kW more exergy may be produced.
c) When the components with highest exergy destruction rate are listed, they are CON 2, VAP 2 and CON 1 for the CExA analysis, CON 2, CON 1 and VAP 2 for the AExA analysis, and VAP 2, CON 2 and CON 1 for the ABC optimization method. Thus the components requiring priority improvement are determined.
d) The highest exergy destruction rate obtained from calculations of the methods used to improve thermodynamic performance of the GPP occurs in heat exchangers (CONs, VAPs).
e) It is worth mentioning that the results of the AExA analysis should be verified with those of ABC optimization method. The reason for this is that the theoretical and unavoidable assumptions in the AExA analysis are linked to the decision maker and are therefore somewhat arbitrary as a single value. In the ABC method, value of each optimized parameter is selected at constraint limits (min and max range). Therefore, its fitness value is determined as estranged from arbitrariness.

Thus to increase the thermodynamic performance of geothermal power plants, similar analysis and numerical simulation studies to this one should be performed and it should be confirmed that the results reflect reality. Therefore, the study and similar studies will ensure a boost to the performance of systems producing power from geothermal and other sources.

Acknowledgments

The authors gratefully acknowledge the support provided for the present work by the Maren Geothermal Inc. and the personal support of, Mr. Ertan Türk. The authors are very grateful to the reviewers due their appropriate and constructive suggestions as well as their proposed corrections, which have been utilized in improving the quality of the paper.

Nomenclature

D	number of parameters to be optimized
$\dot{E}x$	exergy rate (kJ/s or kW)
h	specific enthalpy (kJ/kg)
$\dot{m}$	mass flow rate (kg/s)
NP	number of colony size
P	pressure (kPa)
$\dot{Q}$	heat transfer rate (kW)
s	specific entropy (kJ/kgK)
SN	number of food sources
T	temperature (°C or K)
$\dot{W}$	work rate, power (kW)
Greek symbols	
Δ	difference
ε	exergy or second law efficiency (%)
φ	random number [-1,1]
ψ	flow exergy (kJ/kg)

Subscripts

D	destruction
F	fuel
in	input
is	isentropic
j	successive number of elements
k	location
L	loss
mech	mechanical
out	output
P	product
sys	system
0	reference state

Superscripts

AV	avoidable
EN	endogenous
EX	exogenous
UN	unavoidable

Abbreviations

ABC	artificial bee colony
AExA	advanced exergy analysis
ANN	artificial neural network
CExA	conventional exergy analysis
CON	condenser
DE	differential evolution
GA	genetic algorithm
GPP	geothermal power plant
NCG	non-condensable gases
ORC	organic Rankine cycle
PRE-HE	preheater
PSA	pattern search algorithm
PSO	particle swarm optimization
PU	pump
RECUP	recuperator
SCADA	Supervisory Control System
TURB	turbine
VAP	vaporizer

References

[1] Melikoglu M. Geothermal energy in Turkey and around the World: a review of the literature and an analysis based on Turkey's Vision 2023 energy targets. Renew Sustain Energy Rev 2017;76:485–92.
[2] Bleicher A, Gross M. Geothermal heat pumps and the vagaries of subterranean geology: energy independence at a household level as a real world experiment. Renew Sustain Energy Rev 2016;64:279–88.
[3] Pfenninger S, Keirstead J. Comparing concentrating solar and nuclear power as baseload providers using the example of South Africa. Energy 2015;87:303–14.
[4] Nicholson M, Biegler T, Brook BW. How carbon pricing changes the relative

competitiveness of low-carbon baseload generating technologies. Energy 2011;36:305–13.
[5] Khublaryan MG. Types and properties of waters. Encyclopedia of life support systems, vol. 1. Oxford, United Kingdom: EOLSS Publishers Co. Ltd.; 2009. p. 1–159.
[6] Bertani R. Geothermal power generation in the world 2010–2014 update report. Geothermics 2016;60:31–43.
[7] TEIAS. Turkish electricity transmission corporation, http://www.teias.gov.tr/, Accessed date: 15.04.2017.
[8] Rosen MA, Dincer I. Exergy methods for assessing and comparing thermal storage systems. Int J Energy Res 2003;27(4):415–30.
[9] Tsatsaronis G. Design optimization using exergoeconomics. In: Thermodynamic optimization of complex energy systems. Dordrecht: Kluwer Academic Publishers; 1999.
[10] Keçebaş A, Gökgedik H. Thermodynamic evaluation of a geothermal power plant for advanced exergy analysis. Energy 2015;88:746–55.
[11] Gökgedik H, Yürüsoy M, Keçebaş A. Improvement potential of a real geothermal power plant using advanced exergy analysis. Energy 2016;112:254–63.
[12] Nami H, Nemati A, Fard FJ. Conventional and advanced exergy analyses of a geothermal driven dual fluid organic Rankine cycle (ORC). Appl Therm Eng 2017;122:59–70.
[13] Dai Y, Wang J, Gao L. Parametric optimization and comparative study of organic Rankine cycle (ORC) for low grade waste heat recovery. Energy Convers Manag 2009;50:576–82.
[14] Sun J, Li WH. Operation optimization of an organic Rankine cycle (ORC) heat recovery power plant. Appl Therm Eng 2011;31:2032–41.
[15] Rashidi MM, Galanis N, Nazari F, Parsa AB, Shamekhi L. Parametric analysis and optimization of regenerative Clausius and organic Rankine cycles with two feed water heaters using artificial bees colony and artificial neural network. Energy 2011;36:5728–40.
[16] Arslan O, Yetik O. ANN based optimization of supercritical ORC- binary geothermal power plant: Simav case study. Appl Therm Eng 2011;31:3922–8.
[17] Arslan O. Power generation from medium temperature geothermal resources: ANN-based optimization of Kalina cycle system-34. Energy 2011;36:2528–34.
[18] Wang J, Yan Z, Wang M, Li M, Dai Y. Multi-objective optimization of an organic Rankine cycle (ORC) for low grade waste heat recovery using evolutionary algorithm. Energy Convers Manag 2013;71:146–58.
[19] Clarke J, McLay L, McLeskey Jr JT. Comparison of genetic algorithm to particle swarm for constrained simulation-based optimization of a geothermal power plant. Adv Eng Inf 2014;28:81–90.
[20] Clarke J, McLeskey Jr JT. Multi-objective particle swarm optimization of binary geothermal power plants. Appl Energy 2015;138:302–14.
[21] Karadas M, Celik HM, Serpen U, Toksoy M. Multiple regression analysis of performance parameters of a binary cycle geothermal power plant. Geothermics 2015;54:68–75.
[22] Sadeghi S, Saffari H, Bahadormanesh N. Optimization of a modified double-turbine Kalina cycle by using Artificial Bee Colony algorithm. Appl Therm Eng 2015;91:19–32.
[23] Saffari H, Sadeghi S, Khoshzat M, Mehregan P. Thermodynamic analysis and optimization of a geothermal Kalina cycle system using Artificial Bee Colony algorithm. Renew Energy 2016;89:154–67.
[24] Proctor MJ, Yu W, Kirkpatrick RD, Young BR. Dynamic modelling and validation of a commercial scale geothermal organic Rankine cycle power plant. Geothermics 2016;61:63–74.
[25] Li H, Hu D, Wang M, Dai Y. Off-design performance analysis of Kalina cycle for low temperature geothermal source. Appl Therm Eng 2016;107:728–37.
[26] Wu C, Wang SS, Jiang X, Li J. Thermodynamic analysis and performance optimization of transcritical power cycles using CO_2-based binary zeotropic mixtures as working fluids for geothermal power plants. Appl Therm Eng 2017;115:292–304.
[27] Ozgener L, Hepbasli A, Dincer I. A key review on performance improvement aspects of geothermal district heating systems and applications. Renew Sustain Energy Rev 2007;11:1675–97.
[28] Bell IH, Quoilin S, Wronski J, Lemort V. CoolProp: an open-source reference quality thermophysical property library. In: ASME ORC 2nd international seminar on ORC power systems, Rotterdam, Netherlands; 2013.
[29] Bell IH, Wronski J, Quoilin S, Lemort V. Pure and pseudo-pure fluid thermophysical property evaluation and the open-source thermophysical property library coolprop. Ind Eng Chem Res 2014;53(6):2498–508.
[30] MathWorks, Matlab, http://www.mathworks.com/products/matlab/, Accessed date: 15.04.2017.
[31] Buckley J. Managing Intelligence A guide for law enforcement professionals. USA: CRC Press; 2013.
[32] Businessdictionary,Xhttp://www.businessdictionary.com/definition/optimization.html, Accessed date: 15.09.2017.
[33] Wolpert DH, Macready WG. No free lunch theorems for optimization. IEEE Trans Evol Comput 1997;1(1):67–82.
[34] Dokeroglu T, Cosar A. A novel multistart hyper-heuristic algorithm on the grid for the quadratic assignment problem. Eng Appl Artif Intell 2016;52:10–25.
[35] Karaboga D. An ideal based on honey bee swarm for numerical optimization, Technical Report – TR06. Kayseri, Turkey: Erciyes University, Engineering Faculty, Computer Engineering Department; 2005.
[36] Karaboga D, Akay B. A comparative study of artificial bee colony algorithm. Appl Math Comput 2009;214(1):108–32.
[37] Morosuk T, Tsatsaronis G. A new approach to the exergy analysis of absorption refrigeration machines. Energy 2008;33:890–907.
[38] Morosuk T, Tsatsaronis G. Advanced exergy analysis for chemically reacting systems - application to a simple open gas-turbine system. Int J Thermodyn 2009;12:105–11.
[39] Morosuk T, Tsatsaronis G. Comparative evaluation of LNG e based cogeneration systems using advanced exergetic analysis. Energy 2011;36:3771–8.
[40] Wang L, Yang Y, Morosuk T, Tsatsaronis G. Advanced thermodynamic analysis and evaluation of a supercritical power plant. Energies 2012;5:1850–63.
[41] Petrakopoulou F, Tsatsaronis G, Morosuk T, Carassai A. Conventional and advanced exergetic analyses applied to a combined cycle power plant. Energy 2012;41:146–52.
[42] Morosuk T, Tsatsaronis G. Advanced exergetic evaluation of refrigeration machines using different working fluids. Energy 2009;34:2248–58.
[43] Morosuk T, Tsatsaronis G, Zhang C. Conventional thermodynamic and advanced exergetic analysis of a refrigeration machine using a Voorhees' compression process. Energy Convers Manag 2012;60:143–51.
[44] Tsatsaronis G, Kelly S, Morosuk T. Endogenous and exogenous exergy destruction in thermal systems. In: Proceedings of the ASME IMECE, Chicago, USA; 2006.
[45] Morosuk T, Tsatsaronis G. How to calculate the parts of exergy destruction in an advanced exergetic analysis. In: Proceedings of the ECOS 2008, Cracow-Gliwice, Poland; 2008.
[46] Kelly S, Tsatsaronis G, Morosuk T. Advanced exergetic analysis: approaches for splitting the exergy destruction into endogenous and exogenous parts. Energy 2009;34:384–91.
[47] Cziesla F, Tsatsaronis G, Gao Z. Avoidable thermodynamic inefficiencies and cost in an externally fired combined cycle power plant. Energy 2006;31:1472–89.
[48] Tsatsaronis G, Park MH. On avoidable and unavoidable exergy destructions and investment costs in thermal systems. Energy Convers Manag 2002;43:1259–70.
[49] Bejan A, Tsatsaronis G, Moran M. Thermal design and optimization. New York: Wiley; 1996.
[50] Tsatsaronis G, Morosuk T. A general exergy-based method for combining a cost analysis with an environmental impact analysis. Part I – theoretical development. In: Proceedings of the ASME IMECE, Boston, Massachusetts, USA; 2008.
[51] Tsatsaronis G, Morosuk T. A general exergy-based method for combining a cost analysis with an environmental impact analysis. Part II - application to a cogeneration system. In: Proceedings of the ASME IMECE, Boston, Massachusetts, USA; 2008.
[52] Hepbasli A, Kecebas A. A comparative study on conventional and advanced exergetic analyses of geothermal district heating systems based on actual operational data. Energy Build 2013;61:193–201.
[53] Ozkan C, Kisi O, Akay B. Neural networks with artificial bee colony algorithm for modeling daily reference evapotranspiration. Irrigat Sci 2011;29:431–41.
[54] Karaboga D, Ozturk C. A novel clustering approach: artificial Bee Colony (ABC) algorithm. Appl Soft Comput 2011;11(1):652–7.
[55] Baykasoglu A, Ozbakir L, Tapkan P. Artificial bee colony algorithm and its application to generalized assignment problem. In: Chan FTS, Tiwari MK, editors. Swarm intelligence: focus on ant and particle swarm optimization. Vienna, Austria: ITech Education and Publishing; 2007.
[56] Karaboga D, Basturk B. A powerful and efficient algorithm for numerical function optimization: artificial bee colony (ABC) algorithm. J Global Optim 2007;39(3):459–71.
[57] Dhahri H, Alimi AM, Abraham A. Designing beta basis function neural network for optimization using artificial bee colony (abc). In: IEEE world congress on computational intelligence Brisbane-Australia; 2012.
[58] Karaboga D, Basturk B. Artificial bee colony (abc) optimization algorithm for solving constrained optimization problems. Found Fuzzy Log Soft Comput 2007;4529:789–98.
[59] Kurban T, Besdok E. A comparison of rbf neural network training algorithms for inertial sensor based terrain classification. Sensors 2009;9:6312–29.
[60] Keçebaş A. Performance and thermo-economic assessments of geothermal district heating system: a case study in Afyon, Turkey. Renew Energy 2011;36(1):77–83.
[61] Keçebaş A, Kayfeci E, Gedik E. Performance investigation of the Afyon geothermal district heating system for building applications: exergy analysis. Appl Therm Eng 2011;31:1229–37.
[62] Kecebas A, Coskun C, Oktay Z, Hepbasli A. Comparing advanced exergetic assessments of two geothermal district heating systems for residential buildings. Energy Build 2014;69:434–41.
[63] Penkuhn M, Tsatsaronis G. A decomposition method for the evaluation of component interactions in energy conversion systems for application to advanced exergy based analyses. Energy 2017;133:388–403.
[64] Holman JP. Experimental methods for engineers. New York: McGraw Hill Inc; 2001.